Liquid Crystals
Publication details, including instructions for authors and subscription information:
http://www.informaworld.com/smpp/title~content=t713926090

Structural phase transformations induced by the addition of decanol to the hexagonal phase of the binary sodium decyl sulphate/water system

Y. Hendrikx[a]; J. Charvolin[a]
[a] Laboratoire de Physique des Solides associé au CNRS, Btiment 510, Université Paris, Sud, Orsay, France

To cite this Article Hendrikx, Y. and Charvolin, J.(1992) 'Structural phase transformations induced by the addition of decanol to the hexagonal phase of the binary sodium decyl sulphate/water system', Liquid Crystals, 11: 5, 677 — 698
To link to this Article: DOI: 10.1080/02678299208029020
URL: http://dx.doi.org/10.1080/02678299208029020

LIQUID CRYSTALS, 1992, VOL. 11, NO. 5, 677–698

Structural phase transformations induced by the addition of decanol to the hexagonal phase of the binary sodium decyl sulphate/water system

by Y. HENDRIKX* and J. CHARVOLIN
Laboratoire de Physique des Solides associé au CNRS, Bâtiment 510,
Université Paris Sud, 91405 Orsay, France

(*Received 8 July 1991; accepted 27 October 1991*)

The hexagonal phase of the sodium decyl sulphate/water system transforms into a lamellar phase on the introduction of decanol. This transformation occurs in several steps. We present here a study of the sequence of the corresponding phase transformations. The various phases are identified according to their textures by optical microscopy. It can be seen that, as the decanol/soap ratio increases the two dimensional hexagonal phase is followed by two dimensional rectangular phases before the one dimensional lamellar phase is reached. The symmetries of the structures of the phases and the shapes of their aggregates of amphiphilic molecules were determined by small angle X-ray and neutron scattering studies (SAXS and SANS). Two rectangular phases with cmm and pgg symmetries show up successively between the hexagonal and lamellar phases. The shape of the aggregates evolves along the sequence in an unexpected manner. In the two dimensional hexagonal phase, the aggregates are cylinders with an isotropic circular section at low decanol/soap ratio, which become anisotropic as this ratio increases, i.e. the aggregates become ribbon-like aggregates. The aggregates keep this shape in the rectangular phases, with changes of size, and also, most probably, in the lamellar phase near the two dimensional rectangular phases where it can be seen that the lamellae are fragmented. The local organization of decanol and sodium decyl sulphate molecules within the ribbon-like aggregates was also investigated by SANS and deuteron magnetic resonance (DMR). The SANS studies show that the two molecules are not distributed uniformly within the aggregates, while the DMR measurements show that both amphiphilic molecules stay anchored at the amphiphile/water interface by their polar heads. It can then be inferred that the decanol molecules are preferably in the regions of lowest interfacial curvature and the sodium decyl sulphate molecules are in the regions of highest interfacial curvature. This study shows that addition of decanol in the hexagonal phase induces deformation of the cylinders into ribbons by a local flattening of the interface. This deformation, which starts already deep within the hexagonal phase, is not associated with a change of symmetry of the structure. It also appears that a further deformation of the ribbons into lamellae is not needed for the rectangular phase to change into the lamellar phase when the decanol content increases. Thus, in this sequence of phases, the symmetry of the aggregates and those of their organization are not necessarily related.

1. Introduction

Many studies have been devoted to the structures of lyotropic liquid crystals in general [1–10]. We focus our attention here on to the structural transformations which occur between the hexagonal and the lamellar structure in a few typical phase diagrams. The earliest reported sequences of phase transformations were observed with increasing amphiphile concentration in binary systems of ionic amphiphilic molecules

---

* Author for correspondence.

in the presence of water [2]. For instance in the potassium palmitate/water system, the sequence is: two dimensional hexagonal phase, two dimensional distorted hexagonal, rectangular and complex hexagonal phases, three dimensional cubic phase and finally one dimensional lamellar phase [3]. More recently, in the sodium dodecyl sulphate/water system, besides the already known two dimensional hexagonal and monoclinic phases, rhombohedral, cubic and tetragonal three dimensional phases have been identified with increasing the soap concentration, before reaching the lamellar phase [9–10]. These sequences are rather complicated. On the other hand the binary system of the non-ionic amphiphile, hexa-ethyleneglycol mono *n*-dodecyl ether in the presence of water, shows a much simpler sequence of phases either with increasing the amphiphile concentration or increasing the temperature. This sequence is: two-dimensional hexagonal phase→three dimensional cubic phase→one dimensional lamellar phase [11, 12].

Thus, if those various sequences are described in terms of interfacial curvatures, the transformation of the hexagonal phase with homogeneous cylindrical interfacial curvature, to the lamellar phase with flat interfacial curvature, goes through several phases with inhomogeneous interfacial curvature in the case of ionic amphiphiles whereas it goes through a single phase with rather homogeneous interfacial curvature in the case of the non-ionic one. This can certainly be related to the fact that ionic amphiphiles may present different degrees of dissociation which originate different interfacial curvatures. In order to test this idea it is necessary to show that there is a correlation between the local value of the degree of dissociation of an ionic amphiphile and that of the interfacial curvature. In the absence of any direct experimental means for such an investigation, we decided to approach this problem for a ternary system with two different amphiphilic species, one ionic, the other non-ionic, in the presence of water. The two amphiphiles can be easily labelled by deuteriation and therefore their respective distribution and location in the aggregates of the phases with known structures can be determined by means of sensitive experiments, namely small angle neutron scattering with the contrast variation method and nuclear magnetic resonance.

We have chosen to study the phase transformations which occur when decanol is added to binary sodium decyl sulphate/water mixtures at room temperature [13–15]. The ternary decyl sulphate/decanol/water phase diagram can be extrapolated from existing data concerning sodium dodecyl sulphate/decanol/water and octyl sulphate/decanol/water phase diagrams [7]. We have not explored systematically the whole diagram but limited ourselves to that part of the phase diagram shown in figure 1. We shall discuss in detail the mesophases and phase transformations which were identified along line A. Along this line the water content (H_2O, 47·55 per cent by weight) and the temperature ($23 \pm 1°C$) are maintained constant and the sodium decyl sulphate molecules are progressively replaced by decanol molecules. The sequence of phases, when the decanol/soap molar ratio increases, appears to be: two dimensional hexagonal phase, two dimensional rectangular phases with different symmetries and finally the one dimensional lamellar phase. The decanol molecules may be seen as the driving force for the phase transformations along this sequence.

2. Experimental

2.1. *Samples*

The samples were prepared in sealed glass tubes mixing together known amounts of sodium decyl sulphate (SdS), 1-decanol (C_{10}–OH) and water. In the case of protonated

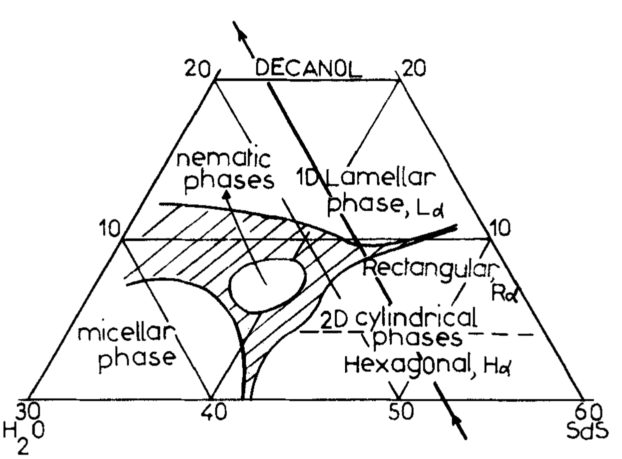

Figure 1. Part of the phase diagram SdS/decanol/water which has been explored at 23 ± 1°C. Concentrations are in weight per cent. The hatched area corresponds to a polyphasic domain.

molecules, SdS and C_{10}–OH were of commercial origin (respectively Merck ppa 99 per cent and Fluka ppa 99 per cent), light water (H_2O) was distilled. Perdeuteriated SdS and C_{10}–OH were prepared in the laboratory by C. Germain from perdeuteriated decanoic acid (CD_3–$(CD_2)_8$–COOH, isotropic content > 99 per cent from 'Service des molécules marquées, CEA Saclay', heavy water (D_2O, 99·8 per cent) was from the same origin.

The tubes were stored in an oven for several days. The temperature of the oven was maintained below 40°C in order to prevent an eventual hydrolysis of SdS into C_{10}–OH. The homogenization of the samples was improved by centrifugation and ultrasonication. The compositions of the samples, together with the C_{10}–OH/SdS molar ratio, r, are given in table 1. The nature of the samples, ordered cylindrical (hexagonal and rectangular) or lamellar phases was first identified by observing their textures with a polarizing microscope [13, 16].

2.2. *X-ray diffraction experiments*

The structures of randomly oriented samples were obtained by small angle X-ray (SAXS) diffraction. We use the following notation $|\mathbf{q}| = 4\pi \sin \theta/\lambda$, where $\mathbf{q}$ is the scattering vector, λ the wavelength and 2θ the angle between the scattered and incident beams. Two experimental devices were used. One was a Guinier camera with linear collimation and either monochromatic Co–K_{α_1} radiation, $\lambda = 1{\cdot}7889$ Å, or monochromatic Cu–K_{α_1} radiation, $\lambda = 1{\cdot}5405$ Å. This camera allows us to investigate a wide range of scattering vectors, $0{\cdot}07\,\text{Å}^{-1} \leqslant |\mathbf{q}| \leqslant 2{\cdot}0\,\text{Å}^{-1}$, with high resolution. The second experimental device is another small angle X-ray scattering one with semi-linear collimation and monochromatic Cu–K_{α_1} radiation, $\lambda = 1{\cdot}5405$ Å, giving access to a smaller scattering vector range, down to $0{\cdot}05\,\text{Å}^{-1}$ and up to $0{\cdot}6\,\text{Å}^{-1}$. In both cases the $|\mathbf{q}|$ values of the Bragg reflections observed at small angles give access to the symmetry and parameters of the unit cell. From these, knowing the concentration and partial molar volume of each component of the sample, a first approximation of the shape and the dimensions of the aggregates of the mesophases can be obtained. For all of the investigated mesophases a diffuse band was observed in the large angle region, which confirms the liquid-like state of the paraffinic chains of the amphiphilic molecules [2].

Table 1. Composition of the sample.

	Weight %			Mole %			
Sample	SdS	C_{10}–OH	H_2O	SdS	C_{10}–OH	H_2O	C_{10}–OH/SdS molar ratio, r
1	52·44	—	47·56	7·09	0	92·91	—
2	51·43	1·03	47·53	6·95	0·23	92·82	0·03
3	50·32	2·12	47·56	6·79	0·47	92·74	0·07
4	49·28	3·15	47·57	6·64	0·70	92·66	0·11
5	48·59	3·88	47·53	6·55	0·86	92·59	0·13
6	48·05	4·42	47·55	6·47	0·98	92·55	0·15
7	47·80	4·63	47·57	6·43	1·03	92·54	0·16
8	47·60	4·83	47·57	6·41	1·07	92·52	0·17
9	47·17	5·26	47·57	6·35	1·16	92·49	0·18
10	46·71	5·71	47·58	6·28	1·26	92·46	0·20
11	46·52	5·90	47·58	6·25	1·31	92·44	0·21
12	46·12	6·31	47·58	6·20	1·39	92·41	0·22
13	45·66	6·79	47·55	6·14	1·50	92·36	0·24
14	45·07	7·37	47·56	6·05	1·63	92·33	0·27
15	41·90	10·54	47·56	5·61	2·32	92·09	0·41
16	41·28	11·09	47·63	5·52	2·44	92·04	0·44
17	37·06	15·33	47·61	4·94	3·36	91·70	0·68
18	35·00	17·44	47·56	4·66	3·82	91·52	0·82
19	30·82	21·63	47·55	4·09	4·72	91·19	1·15
20	20·25	32·12	47·62	2·66	6·94	90·40	2·63
21	18·20	34·28	47·52	2·39	7·41	90·20	3·10
22	16·10	36·40	47·49	2·11	7·85	90·03	3·72

The experiments were carried out at 23 ± 1°C. The samples were held between mica sheets separated by a teflon spacer, thickness 0·7 mm, in a cell whose tightness was ensured by a set of joints and mechanical clamping.

2.3. *Neutron scattering experiments*

2.3.1. *Monocrystalline samples of the lamellar phase*

Oriented samples are needed to obtain a complete picture of reciprocal space in order to locate eventual diffuse scatterings with respect to the Bragg reflections. Monocrystalline domains of the lamellar phase were obtained by squeezing or flowing the phase between closely spaced parallel glass plates [17]. X-rays are strongly absorbed by glass but quartz plates are transparent to neutrons. We have chosen, therefore, to work with quartz plates when using neutron scattering. The experiments were performed on spectrometer D17 equipped with a XY multidetector at Institut Laue Laugevin (ILL), Grenoble. The scattering vectors range along the director, **n**, of the phase was $0·02\,\text{Å}^{-1} \leqslant |\mathbf{q}| \leqslant 0·2\,\text{Å}^{-1}$. We worked with protonated SdS and C_{10}–OH in D_2O so that the scattered intensity depends on the contrast of the amphiphilic molecules with respect to D_2O and therefore on the relative distribution of amphiphiles and water and not on that of soap and alcohol. The experiments were carried out at 23 ± 1°C.

2.3.2. *Contrast variation experiments on phases with cylindrical aggregates*

Coherent scattering of neutrons is much stronger for deuterons than for protons and this can be used to study the relative distribution of two molecules when one is deuteriated while the other is kept protonated. We have already described this method in other papers [15, 18, 19]; we now briefly recall its principle. If on the one hand, the distribution of the species within the aggregates is uniform, the aggregates will have a uniform scattering length density corresponding to the average value of the scattering length densities of the deuteriated and protonated aliphatic chains. If, on the other hand, the distribution of the species is not uniform, the scattering length density of the aggregate will be modulated according to the distribution of the molecules, the amplitude of this modulation being limited to the difference between the scattering length densities of the deuteriated and protonated chains. The form factor of the aggregates will, therefore, be different in the two cases, and for mesophases with long range translational order the intensities of the Bragg reflections should be modulated differently. Moreover, we can control another parameter which may help to discriminate between both situations: the contrast of the aggregate with respect to the surrounding solvent which depends on the scattering length density of the latter. Thus, if the distribution of deuteriated and protonated amphiphiles is homogeneous, the spectra obtained for a mesophase made of aggregates in H_2O or in D_2O must be similar and the ratio between the intensities of all the corresponding Bragg reflections must be the same, i.e. it will scale the solvent variation. This will not be the case if the distribution of both amphiphilic molecules is not uniform.

The interfacial region of the aggregates, where the polar heads are localized constitutes an heterogeneity which might be the source of a phenomenon similar to the one just discussed. A contrast variation study of aggregates with protonated amphiphiles (potassium laurate and 1-decanol) has shown that the contribution of the polar heads is negligible [20]. However, for the development of a model of structure factor calculation, it is easier to work in conditions such that the scattering length density of the solvent matches those of the polar heads. Therefore, some samples were prepared with a mixture of light and heavy water (26 per cent H_2O and 74 per cent D_2O) whose scattering length density, $\rho_S = 4{\cdot}59\,\mathrm{cm}^{-2} \times 10^{10}$, matches those of the polar head groups of the amphiphilic molecules which are respectively $4{\cdot}33 \times 10^{10}\,\mathrm{cm}^{-2}$ for the OSO_3Na group and $4{\cdot}62 \times 10^{10}\,\mathrm{cm}^{-2}$ for the hydroxyl group (taking into account the isotopic exchange OH/OD). For these experiments we prepared samples with the same molar composition but different states of deuteriation.

They were made either of protonated SdS and C_{10}–OH or of protonated SdS and deuteriated C_{10}–OH in the mixture of light and heavy water. The scattering length density of the samples with fully protonated aggregates cannot but be uniform. On the other hand the scattering length density of the samples with protonated SdS and deuteriated C_{10}–OH can be, as we have outlined, either uniform or not. The form factor of the aggregates are different in these two last situations. In the first situation, when the distribution is homogeneous, the intensity of the Bragg reflections of a sample with deuteriated C_{10}–OH and that of the sample with the same C_{10}–OH/SdS ratio with protonated amphiphiles will simply scale the difference between the scattering length density of the protonated aggregates and that of the partially deuteriated ones, i.e. if ρ_1 is the scattering length density of fully protonated aggregates, $\bar{\rho}_2$, the average scattering length density of partially deuteriated aggregates, ρ_s being that of the solvent, the scattered intensity, $I(\mathbf{q})$, will be proportional to $(\rho_1 - \rho_s)^2$ and to $(\bar{\rho}_2 - \rho_s)^2$ respectively ($\rho_1, \bar{\rho}_2, \rho_s$ can be calculated from the compositions of the samples and the tables of scattering length densities given in table 2). In the second situation, when the distribution is inhomogeneous, the intensity of the Bragg reflection of a sample with perdeuteriated C_{10}–OH and that of the sample with the same C_{10}–OH/SdS molar ratio

Table 2. Scattering length densities, ρ.

Protonated species and sulphate group	$\rho/10^{10}\,\mathrm{cm}^{-2}$	Deuteriated species	$\rho/10^{10}\,\mathrm{cm}^{-2}$
H_2O	−0·56	D_2O	6·39
CH_2	−0·31	CD_2	7·43
CH_3	−0·85	CD_3	4·93
CH_3–$(CH_2)_9$–	−0·41	C_3–$(CD_2)_9$–	6·97
O–SO_3Na	4·29		
OH	0·94	OD	5·70
Protonated SdS	0·48	Deuteriated SdS	6·19
Protonated C_{10}–OH	−0·31	Deuteriated C_{10}–OH	6·24

with protonated amphiphiles will not simply scale the difference between $(\rho_1-\rho_s)^2$ and $(\bar{\rho}_2-\rho_s)^2$.

The patterns were obtained with spectrometer D_1B at ILL, Grenoble, equipped with a linear multidetector or with spectrometer PAXY of Laboratoire Leon Brillouin (LLB) CEN-Saclay, equipped with a XY multidetector; the scattering vectors range were respectively $0{\cdot}05\,\text{Å}^{-1}\leqslant|\mathbf{q}|\leqslant 1\,\text{Å}$ and $0{\cdot}04\,\text{Å}^{-1}\leqslant|\mathbf{q}|\leqslant 0{\cdot}4\,\text{Å}^{-1}$. We worked with randomly oriented samples contained in quartz cells 1 mm thick and the experiments were carried out at 23 ± 1°C. The data were normalized for unit incident beam flux and corrected for background, absorption and detector efficiency. In all cases we ensured, by X-ray scattering studies, that the structure and structural parameters of the samples are independent of the percentages of deuteriated molecules.

2.4. *Structure factor calculation: characterization of the normal section of the aggregates*

The spacings of the Bragg reflections on an X-ray or neutron diffraction pattern give access to the structure of the mesophase investigated and to the dimensions of the unit cell. The relative intensities of these reflections are relevant to the shape and the internal structure of the aggregates of the unit cell. However, this information is not directly available. In principle, knowledge of the scattered amplitudes at the reciprocal lattice points allows, via the inverse Fourier transform, to go back to the scattering length density profile of the unit cell and thus to the shape and internal structure of the aggregates. However, in the present study, this problem is not easy to solve. Due to the rapid decrease of the form factor of the aggregates, a limited number of reflections are observed and apart from the fact that the determination of the phase of the reflections is difficult, for lack of a sufficient number of reflections, the inverse Fourier transform on a truncated reciprocal space will not describe the unit cell in a satisfactory way. Therefore, the problem has been reversed: a model of the unit cell is built, i.e. we assume the scattering length density $\rho(\mathbf{r})$ is known. The intensities of each of the Bragg reflections are calculated by Fourier transform and these intensities are compared with those of experimental spectra and the model is modified up to the best fit with the experimental results. Therefore, for the rectangular phase with pgg symmetry, we have used a program of structure factor calculation which allows us when the structural parameters of the unit cell and the composition of the motif are known to calculate the scattered intensities at the points of the reciprocal lattice [21]. The usual correction factors peculiar to diffraction experiments (reflections multiplicity, Lorentz factor, polarization factor, except the Debye–Waller factor because, on the one hand, it is difficult to estimate in the systems investigated, and on the other, it becomes particularly important at large scattering vectors which are not reached here) and the instrumental signal to noise ratio were taken in account, to compare the intensities of the reflections of the calculated pattern with those of the experimental one for different shapes and dimensions of the normal section of the aggregates of the phase investigated. The easiest way to proceed is to determine the shape and the dimensions of the normal section of aggregates whose scattering length density is uniform. This is achieved when the aggregates are fully protonated and the scattering length density of the surrounding solvent matches that of the polar heads (neutron scattering experiments). The calculated pattern will fit the experimental one for a particular shape and dimensions of the section of the aggregates and a given tilt angle of the latter with respect to the unit cell. Then, with the adequate shape, the second step should consist in looking for the distribution of both amphipiles in the aggregates, i.e. to determine their internal structure. Therefore the pattern of a sample with the same molar composition as the fully protonated one, but this time with protonated soap and deuteriated decanol was recorded.

2.5. *DMR experiments*

In addition to neutron scattering experiments, DMR measurements were performed in order to discriminate between different possible environments of the decanol molecules. The magnitudes and the gradient of the quadrupolar splittings of deuteriated methylene and methyl groups along the hydrocarbon chain of an amphiphilic molecule depend on the order parameters of the chain links, or the conformational state of the chain, and therefore reflects the situation of the molecule relative to the interface and its environment.

We expect that the organisation of the decanol molecules relative to the normal to the interface is similar to that of the soap molecules, this means with their hydroxyl heads at the interface and in such a situation, the quadrupolar splittings associated with the chain links of the decanol molecules should be similar to those of the SdS molecules. However, it might be imagined that the decanol molecules have their hydroxyl group in the core of the aggregates, but this situation is highly improbable, or that they are randomly solubilized in this core. In this latter case the decanol molecules would behave as alkane molecules and the quadrupolar splittings, particularly those associated to the methylene groups in the vicinity of the polar heads, would be about a factor of ten lower than the corresponding ones of the paraffinic chains of the SdS molecules [22].

The deuteron quadrupolar splittings of SdS deuteriated chains and those of C_{10}–OH deuteriated chains in samples with the same molar composition but with protonated C_{10}–OH in the first case and protonated SdS in the second case were recorded for SdS/C_{10}–OH/water samples of the hexagonal, rectangular (pgg) and lamellar phases. The measurements were made at 25°C with a Bruker spectrometer CXP 100 equipped with a Drusch electromagnet of 2·1 T.

3. Results

3.1. *Structures*

The equations that define the spacing of the reflections for the different symmetry with periodicities along one or two dimensions which have been observed along line A of the phase diagram shown in figure 1 are [23]

(i) Periodic in two dimensions: hexagonal, space group: p6m

$$q_{hk} = 2\pi a^*(h^2 + k^2 - hk)^{1/2}$$

(ii) Periodic in two dimensions: rectangular

(a) space group cmm

$$q_{hk}=2\pi(h^2a^{*2}+k^2b^{*2})^{1/2}\quad (h+k=2n)$$

(b) space group pgg

$$q_{hk}=2\pi(h^2a^{*2}+k^2b^{*2})^{1/2}\quad (ho=2n; ok=2n)$$

(iii) Periodic in one dimension: lamellar

$$q_l=2\pi l/d$$

with q_{hkl} reciprocal spacing of the reflection with indices h, k and l, a^*, b^* the dimensions of the reciprocal unit cell, and d the repeat distance of the lamellar phase.

The symmetry of the lattice is determined by finding out which equation fits the observed spacings. When the symmetry is found, the dimensions of the unit cell can be calculated. The structure and lattice parameters of the samples along line A of the phase diagram sketched in figure 1 are given in table 3.

3.1.1. *The hexagonal phase*

The X-ray powder patterns of the hexagonal phase, all show two or three narrow Bragg reflections whose positions are in the ratio $1, \sqrt{3}, \ldots$, which corresponds to the packing of infinite cylinders on a two-dimensional hexagonal lattice. When the cylinders are embedded in a continuous water medium the phase is called direct or type I hexagonal phase, H_α (in Luzzati's notation [23]). The position of the first order is $d\sqrt{3}/2$, where d is the lattice parameter. From d we can deduce the diameter, d_a, of the cylinders according to the relation [2]

$$d_a=d\left[\frac{2/\sqrt{3}}{\pi}\,\frac{1}{1+\bar{v}_e/\bar{v}_a x(1-C)/C}\right]^{1/2},$$

where C is the weight concentration of the amphiphile, for one gram of the mixture, $\bar{v}_e$ and $\bar{v}_a$ are the partial molar volumes of the solvent and the amphiphile respectively.

The radius of the aggregates, R, is plotted versus the decanol concentration, in mole per cent, in figure 2. As already reported [19], R increases when the C_{10}–OH/SdS molar ratio, r, increases. The lattice is hexagonal for $0=r\leqslant 0{\cdot}15$.

3.1.2. *The rectangular phases*

For C_{10}–OH/SdS molar ratios, $r>0{\cdot}15$, the hexagonal phase transforms into a rectangular phase of space group cmm. This phase extends over a narrow decanol concentration domain, $0{\cdot}16\leqslant r\leqslant 0{\cdot}18$, and transforms rapidly in a rectangular phase, R_α, of space group pgg which extends for, $0{\cdot}20\leqslant r\leqslant 0{\cdot}27$.

Typical diffraction patterns of rectangular phases of space group cmm and pgg are shown in figures 3 (*a*) and (*b*), respectively. The indexation of the reflections are reported in table 4. Between both rectangular phases, a two phase region exists which, according to the possible indexations of the diffraction patterns, must be a mixture of both rectangular, cmm and pgg, phases.

Figure 4 illustrates that the hexagonal lattice (one aggregate per unit cell) fits with a centred rectangular phase (two aggregates per unit cell). This allows us to describe the evolution of the hexagonal lattice to the rectangular one. When the ratio b/a is no

Table 3. SAXS experiments. Structure and lattice parameters of the samples.

Sample	C_{10}–OH/SdS molar ratio, *r*	Structure	*d*/Å†	*a*/Å	*b*/Å
1	—	H_α, p6m	40·04	—	—
2	0·03	↑	40·15	—	—
3	0·07	│	41·64	—	—
4	0·11	│	42·32	—	—
5	0·13	↓	42·63	—	—
6	0·15	H_α, p6m	43·11	—	—
7	0·16	R_α, cmm	—	37·5	109·0
8	0·17	↕	—	36·6	114·0
9	0·18	R_α, cmm	—	38·2	99·5
10	0·20	R_α, pgg	—	37·2	120·0
11	0·21	↑	—	37·4	107·0
12	0·22	│	—	38·3	111·0
13	0·24	↓	—	38·5	103·6
14	0·27	R_α, pgg	—	37·8	117·0
15	0·41	L_α	37·2	—	—
16	0·44	↑	36·9	—	—
17	0·68	│	42·4	—	—
18	0·82	│	47·7	—	—
19	1·15	│	46·9	—	—
20	2·63	│	45·7	—	—
21	3·10	↓	46·3	—	—
22	3·72	L_α	47·4	—	—

† *d*/Å, lattice parameter of the H_α phase and periodicity of the L_α phase.

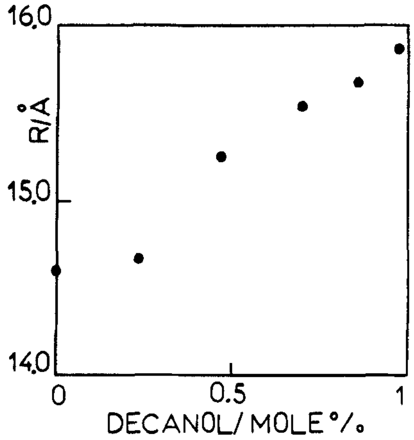

Figure 2. Radius of the aggregates, *R*, as a function of the decanol concentration.

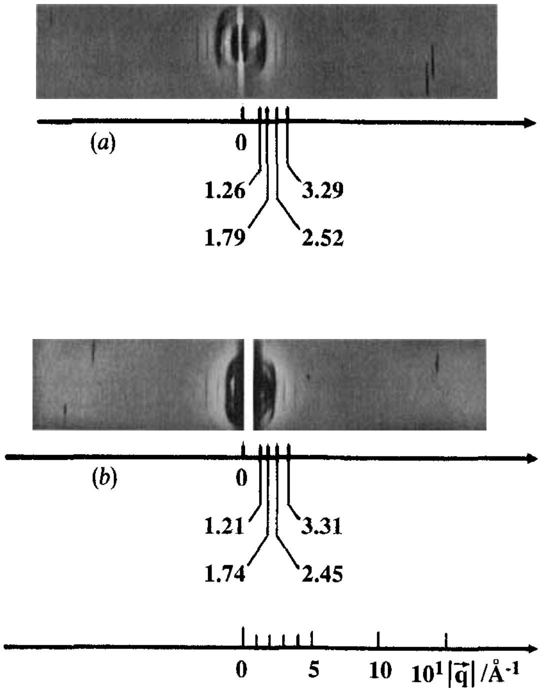

Figure 3. Diffraction patterns of rectangular phases obtained with a Guinier camera: (*a*) sample 9, rectangular, space group cmm; (*b*) sample 13, rectangular, space group pgg.

Table 4. Indexation of the reflections of the patterns shown in figure 3.

Figure 3(*a*), sample 9, rectangular, space group cmm			Figure 3(*b*), sample 13, rectangular space group pgg		
h	k	$q\times 10$ Å^{-1}	h	k	$q\times 10$ Å^{-1}
0	2	1·26	0	2	1·21
1	1	1·79	1	1	1·74
0	4	2·53	1	3	2·45
2	0	3·29	2	1	3·31

longer $\sqrt{3}$ (characteristic of the hexagonal lattice), the six fold symmetry is lost and the hexagonal phase transforms into a rectangular one with $b/a \simeq 3$.

3.1.3. *The lamellar phase*

When r is further increased a polyphasic domain, which will not be discussed here, is crossed before the lamellar domain is reached for $r=0·41$. The diffraction patterns of randomly oriented samples along line A for $0·41<r=3·72$ (the upper limit so far studied), are characterized by a set of narrow Bragg reflections in the ratio 1, 2, 3,... The classic description of a lamellar L_α phase of amphiphilic molecules in the presence of water is that of a periodic stacking along one dimension of infinite flat amphiphilic bilayers separated by water layers. If the periodicity of the lamellar stacking, d, is plotted versus the molar decanol content (see figure 5), two domains are observed: in one periodicity increases until the decanol content reaches a value equal to 3·82 mole

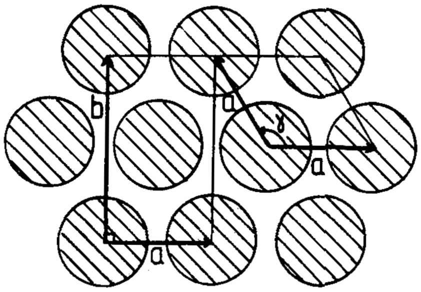

Figure 4. Primitive hexagonal unit cell and centred rectangular one associated with the hexagonal lattice.

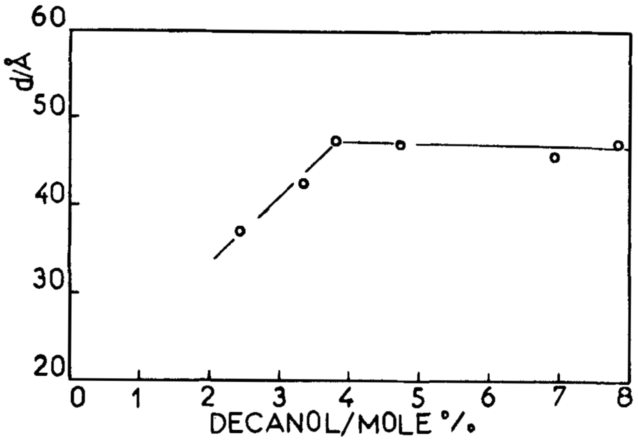

Figure 5. Periodicity of the lamellar phase, *d*, as a function of the decanol concentration.

per cent; thereafter, in the second periodicity remains constant. This behaviour is unusual. However in the last few years X-ray and neutron scattering studies on oriented samples have suggested that some lamellar phases migh have complex structures [24–26]. We could infer from a diffraction pattern shown in figure 6 (decanol content equal to 2·32 mole per cent) which shows a diffuse scattering band for a scattering vector $|\mathbf{q}| \sim 0{\cdot}08$ Å^{-1}, that the structure of the lamellar phase investigated deviates from the classical one. In order to locate the diffuse scattering with respect to the Bragg reflections, we have performed a neutron scattering study on oriented samples of the lamellar domain. The results of this study, quoted in [27], show that when $r < 0{\cdot}82$, the amphiphilic bilayers are not homogeneous.

3.2. *Shape of the aggregates associated with the different structures*

3.2.1. *Aggregates of the hexagonal phase*

This phase is made of infinite cylinders which are generally described as having circular sections. Two arguments are in favour of this description, when the cylinders are aggregates of amphiphilic molecules. One is that the area of the section determined from X-ray scattering experiments is that of a circle having a radius in general less than the length of an extended amphiphilic molecule. The second is that sections with symmetries higher than six are compatible with the p6m symmetry of the lattice. When SdS molecules are progressively replaced by C_{10}–OH the radius of the cylinders of the hexagonal phase becomes larger than the molecular length (see figure 2) and hence the

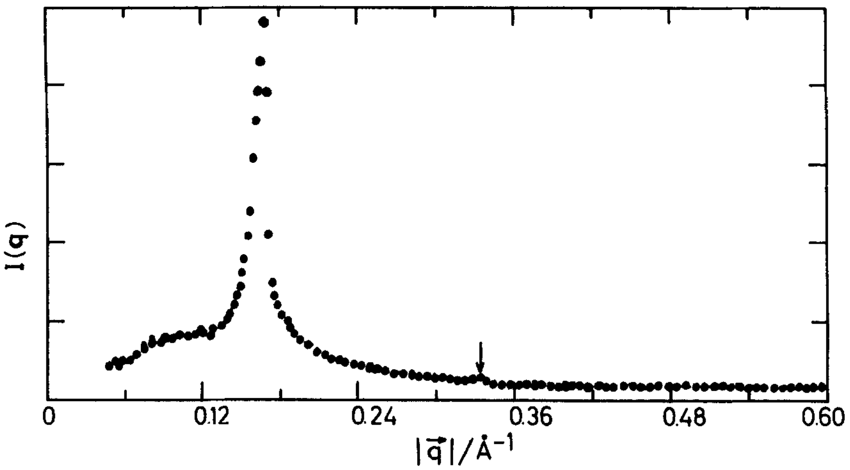

Figure 6. Diffraction pattern of the lamellar phase corresponding to sample 15. Diffuse scattering besides the Bragg reflections is observed.

area of the section of the cylinders increases progressively. This growth of the section could be isotropic or anistropic. We have solved this question which cannot be answered by X-ray scattering alone. We have, therefore, applied an approach similar to that used to detect a local biaxiality in a lyotropic nematic phase [20].

We have sought to determine the internal structure of the aggregates, or the way the two amphilic molecules are organized within them. We have, therefore, performed neutron scattering experiments applying the contrast variation method [19]. From these experiments we know the soap and decanol molecules are not homogeneously distributed within the aggregates, but this might result either from a solubilization of the decanol molecules within the core of the aggregates, or from an inhomogeneous distribution of the two amphiphilic species along their interface. These two situations correspond to different environments of the molecules and in order to dicriminate between both, we have performed DMR experiments. The latter show (see figure 7 (*a*)) that the conformational state of the paraffinic chains of both molecules is the same, i.e. the organization of the paraffinic chains of the decanol molecules relative to the normal to the interface is similar to that of the soap molecules. We may dismiss the situation where the decanol molecules have their hydroxyl group in the centre of the aggregates because it would be at the origin of a structural heterogeneity in the core of the aggregates, which we could not detect by contrast variation studies performed to determine the internal structure of micelles in a system quite similar to that studied here [20]. From the two sets of experiments it follows that both molecules are arranged similarly to the interface (DMR), but not uniformly distributed along it (neutron scattering); therefore the relative concentrations of hydroxyl and sulphate groups are modulated along the interface, hence the mean area per molecular chain at the interface. Such a modulation is associated with a modulation of the interfacial curvature [14, 15]. The cross section of the cylinders are, therefore, not circular and, the growth of the section with the increase of the decanol/soap ratio is anisotropic.

This phenomenon is important in order to understand the polymorphism of the SdS/C_{10}–OH/H_2O system. When the anisotropy of the section becomes too high, the six-fold symmetry imposed by the hexagonal lattice is not preserved and the hexagonal lattice transforms into a rectangular one.

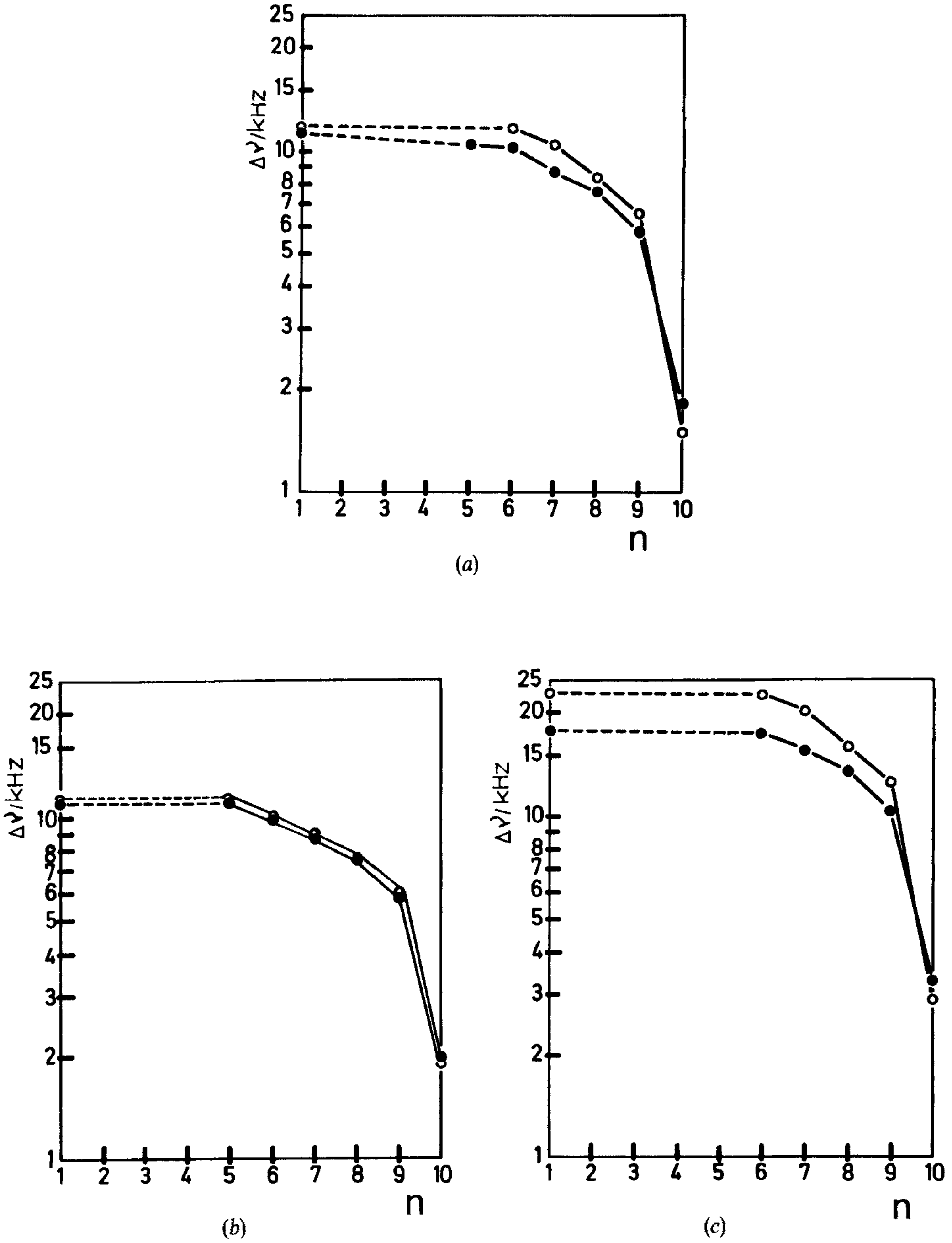

(*a*)

(*b*)

(*c*)

Figure 7. DMR measurements at 25°C. (*a*) Sample 4, hexagonal, H_α phase. (*b*) Sample 12, rectangular, R_α phase, space group pgg. (*c*) Sample 16, lamellar, L_α phase. Quadrupolar splittings $\Delta\nu$, of the CD_2 and CD_3 groups as a function of the carbon number *n* of the methylene group along the chain from the polar head: ●, deuteriated SdS (protonated C_{10}–OH); ○, deuteriated C_{10}–OH (protonated SdS).

3.2.2. *Aggregates of the rectangular phases*

The unit cell contains two aggregates. From the lattice parameters, the molar fractions and the partial molar volumes of the solvent and the amphiphiles, we can calculate the area which corresponds to the cross section of one aggregate in the plane of the unit cell and the dimensions of the cross section can be estimated (thickness $\simeq 19$ Å and width ≈ 52 Å) [13]. The aggregates may be depicted as infinite ribbons with non-circular section.

We have determined precisely the shape of the paraffinic section of the ribbons in a pgg rectangular phase. Therefore, we have used a pattern obtained by neutron scattering of a pgg rectangular phase made of fully protonated soap and decanol in a solvent whose scattering length density matches that of the polar heads (see figure 8 (*a*)). The scattering length density of such a sample cannot but be uniform (see § 2.3.2) and the intensities of the reflections which in such a case are relevant to the shape of the

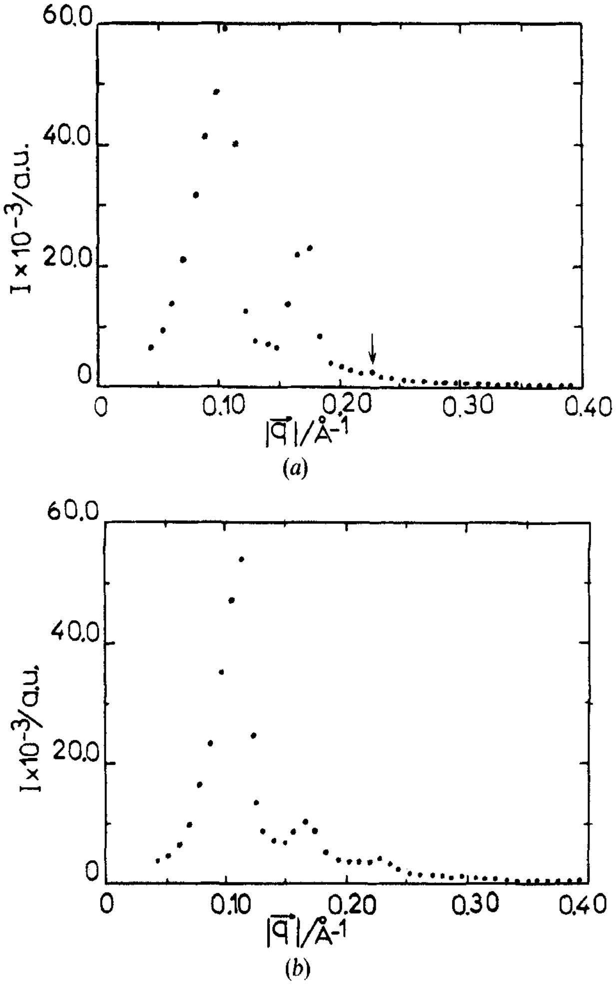

Figure 8. Neutron scattering patterns of the rectangular phase, space group pgg, molar composition, sample 12: (*a*) protonated soap and protonated decanol in 74 per cent D_2O (mole per cent), (*b*) protonated soap and deuteriated decanol in 74 per cent D_2O (mol per cent).

aggregates only, are compared with the intensities of calculated patterns obtained with a program to calculate structure factors (see § 2.4) for different shapes (rectangular, elliptic, rectangular central part capped with two circular parts) and dimensions of the paraffinic section of the aggregates. The best fit is obtained for a section with a rectangular central part capped with two circular parts, i.e. formed by a rectangular part, 25 Å length and 19 Å width, capped with two circular parts with radius 12·5 Å as sketched in figure 9, and a tilt angle of the aggregates with respect to the unit cell axis of about 9°, as shown in figure 10.

3.2.3. *Aggregates of the lamellar phase*

Our neutron scattering experiments on oriented samples of the lamellar phase show that diffuse scatterings occur around the Bragg reflections and away from them, which indicate that the structure of this lamellar phase deviates from that usually proposed (see § 3.1.3) [27]. The nature of the deviations depends on the C_{10}–OH/SdS molar ratio. When $0{\cdot}82 \leqslant r \leqslant 3{\cdot}72$ the structure of the phase approaches that usually proposed for lyotropic lamellar phases. The phase is made of infinite homogeneous amphiphilic lamellae separated by water sheets (the periodicity of the lamellar phase is nearly constant (see figure 5). When r decreases ($r = 0{\cdot}68$), in the middle of the lamellar domain, diffuse scattering is observed around the origin (see figure 11 (*a*)) which indicates that the amphiphilic lamellae are affected by the presence of water regions which may be pores or channels piercing them and which are randomly distributed. When $r = 0{\cdot}44$, near the boundary of the lamellar domain, i.e. in the vicinity of the polyphasic domain,

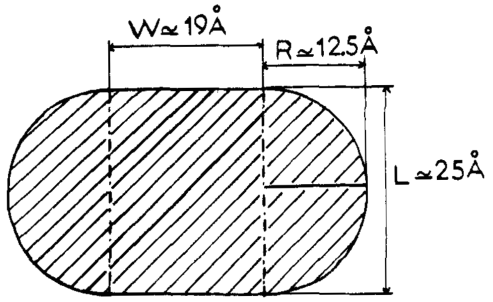

Figure 9. Representation of the paraffinic section of a ribbon-like aggregate of the rectangular pgg phase, sample 12.

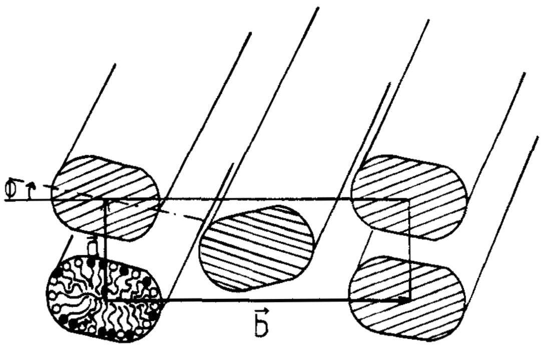

Figure 10. Average representation of the unit cell of a rectangular phase, space group pgg; ● ~, decanol; ○ ~, SdS; $\phi \approx 9°$.

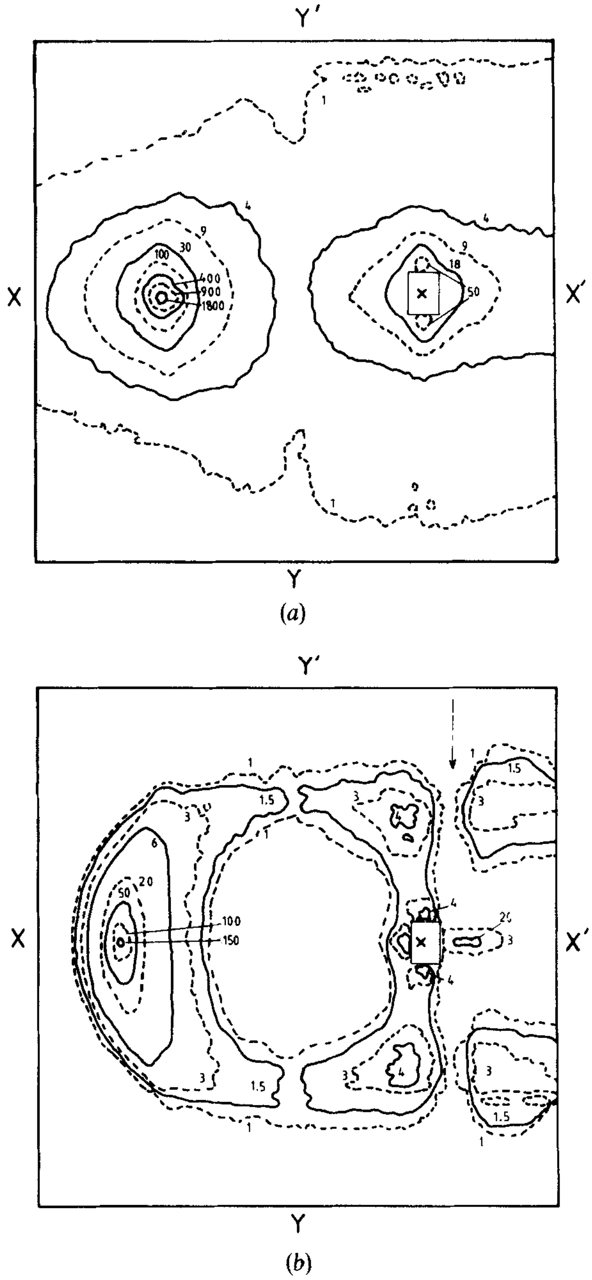

Figure 11. (*a*) Neutron scattering pattern obtained with sample 17, $r = 0{\cdot}68$. Besides the diffuse scattering around the Bragg reflection [27], diffuse scattering is observed around the origin; its intensity increases when $\mathbf{q} \to 0$. (*b*) Neutron scattering pattern obtained with sample 16, $r = 0{\cdot}44$. Diffuse scattering streaks are observed along $\mathbf{q}_\perp$ (perpendicular to the director of the phase); their intensity profile is modulated. The intensity levels are in arbitrary units.

these density fluctuations affect all the lamellae and these water regions are correlated within a lamella and from lamella to lamella over limited regions. This is illustrated by the diffraction pattern shown in figure 11 (*b*): diffuse lateral scattering streaks are observed along $\mathbf{q}_\perp$, i.e. in the plane perpendicular to the director of the phase; moreover, the intensity profile of these streaks is modulated. These water regions must be associated with highly curved interfacial amphiphilic/water boundaries within the lamellae. Moreover, the fact that these water regions show some local organization suggests that they are reminiscent of the structure of the neighbouring rectangular phase made of infinite amphiphilic ribbons embedded in a continuous water medium.

3.3. *Distribution of the amphiphilic molecules within the aggregates*

We have shown qualitatively that the decanol and soap molecules do not distribute themselves uniformly along the interface of the aggregates of the hexagonal phase [19]. This phenomenon is the more enhanced in the rectangular phases. The pattern of the pgg phase made of protonated soap and deuteriated decanol and same molar composition as that of the phase whose pattern is shown in figure 8 (*a*) (with fully protonated amphiphiles) is shown in figure 8 (*b*). If we compare the intensities of the orders of pattern 8 (*a*) with those of the corresponding orders of pattern 8 (*b*), we observe that the first orders are in the ratio 1.1, the second orders in the ratio 2.4 and the third ones in the ratio 0·8. The two patterns are therefore not similar, the form factor of the partially deuteriated aggregates is different from that of the fully protonated one. We can conclude, therefore, as reported in [15], that the distribution of the molecules within the aggregates is not homogeneous.

The non-uniform distribution of both amphiphiles in the pgg rectangular phase is also illustrated in the patterns obtained with either SdS or C_{10}–OH deuteriated in 100 per cent light or 100 per cent heavy water. The corresponding patterns are shown in figures 12 (*a*), (*b*), (*c*) and (*d*). We see from the ratios between the several orders as just discussed, that the patterns (*a*) and (*b*) and (*c*) and (*d*) are not homothetic. These results confirm those outlined in [15]. When the scattering length density of the solvent is varied, different parts of the aggregates are matched and this can only be the case if the distribution of both amphiphiles is not homegeneous.

We may infer from DMR studies of a pgg phase, with either deuteriated SdS molecules and protonated C_{10}–OH molecules or protonated SdS molecules and deuteriated C_{10}–OH molecules, that the conformational state of the paraffinic chains of both amphiphilic molecules is the same. The measured quadrupolar splittings, $\Delta\nu$, of CD_2 and CD_3 groups as a function of the carbon number of the methylene group along the chains are shown in figure 7 (*b*). The quadrupolar splittings for the paraffinic chains of both amphiphiles are very similar. The conformational state of the paraffinic chains of the decanol molecules is analogous to that of the soap molecules and reveals a similar organization of the molecules relative to the normal to the interface (see § 3.2.1). (This holds also for the decanol and soap molecules in the lamellar phase; the corresponding DMR spectrum is shown in figure 7 (*c*).)

The next step would involve determining which molecule, SdS or decanol is preferentially located in the flattened parts of the aggregates. Looking to the sequence sketched in figure 13, it appears that the addition of decanol lowers the mean interfacial curvature, and we may infer that the decanol molecules should be located preferentially in the flattened core of the ribbons and, consequently, that the concentration of the SdS should be higher along their edges.

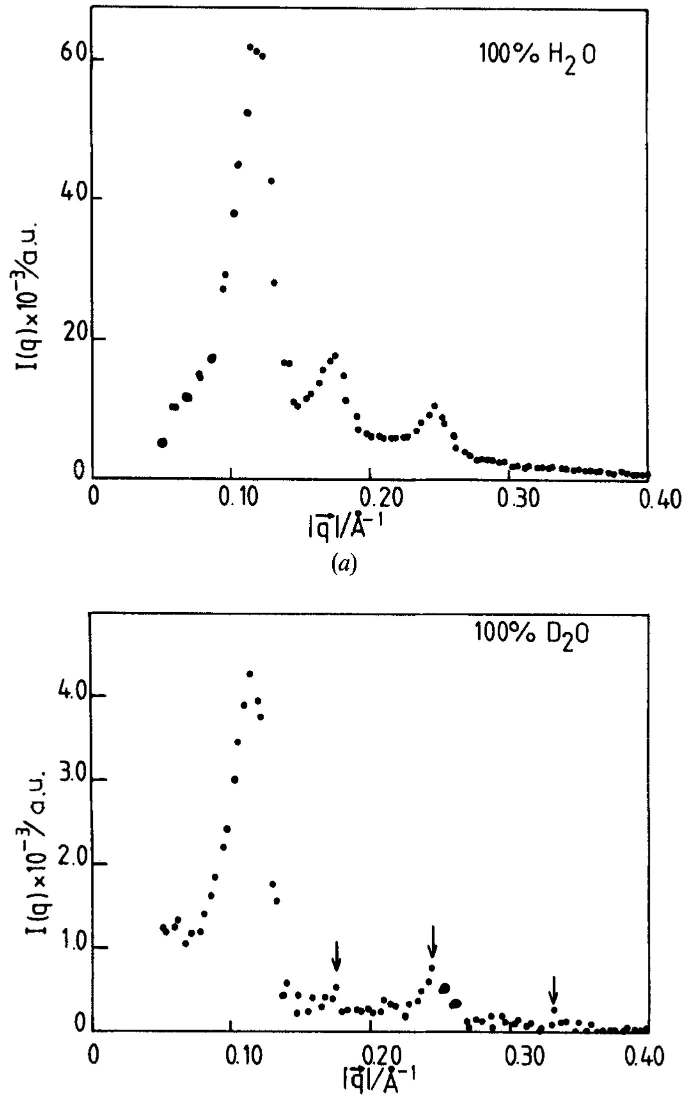
100% H_2O
$I(q) \times 10^{-3}$/a.u.
0
20
40
60
0
0.10
0.20
0.30
0.40
$|\vec{q}|/\text{Å}^{-1}$
100% D_2O
$I(q) \times 10^{-3}$/a.u.
0
1.0
2.0
3.0
4.0
0
0.10
0.20
0.30
0.40
$|\vec{q}|/\text{Å}^{-1}$

(a)

(b)

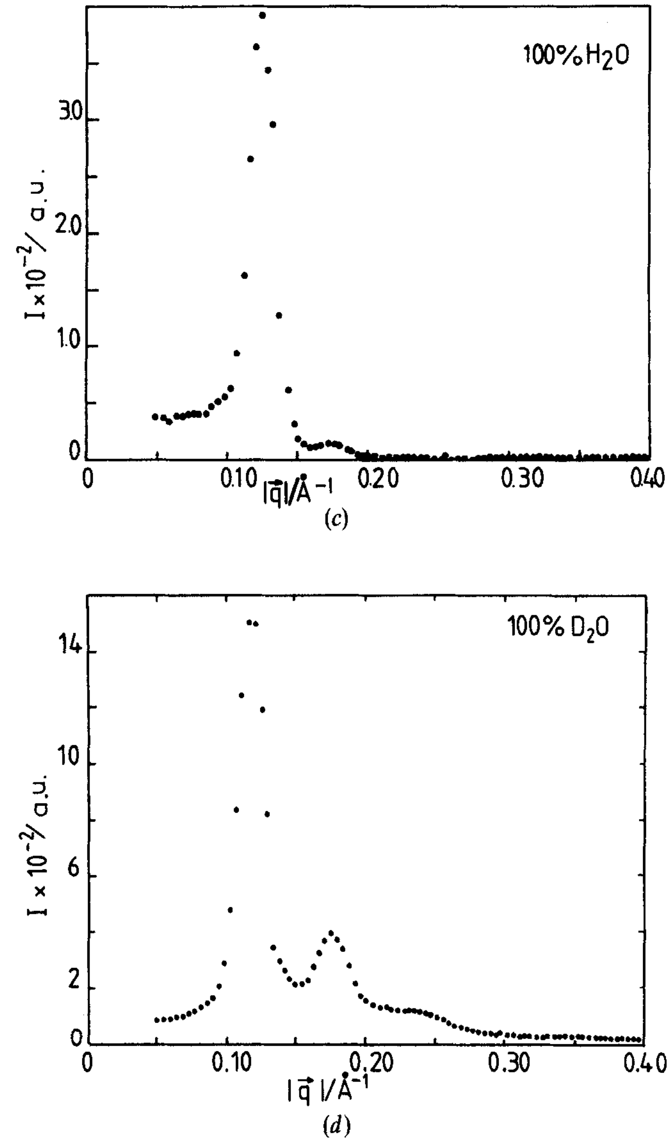

Figure 12. Neutron diffraction patterns of the rectangular phase, space group pgg, molar composition, sample 12: (*a*) deuteriated SdS and protonated decanol in 100 per cent H_2O, (*b*) deuteriated SdS and protonated decanol in 100 per cent D_2O, (*c*) protonated SdS and deuteriated decanol in 100 per cent H_2O, (*d*) protonated SdS and deuteriated decanol in 100 per cent D_2O; (*a*) and (*b*): spectrometer D1B (ILL). (*c*) and (*d*): spectrometer PAXY (LLB).

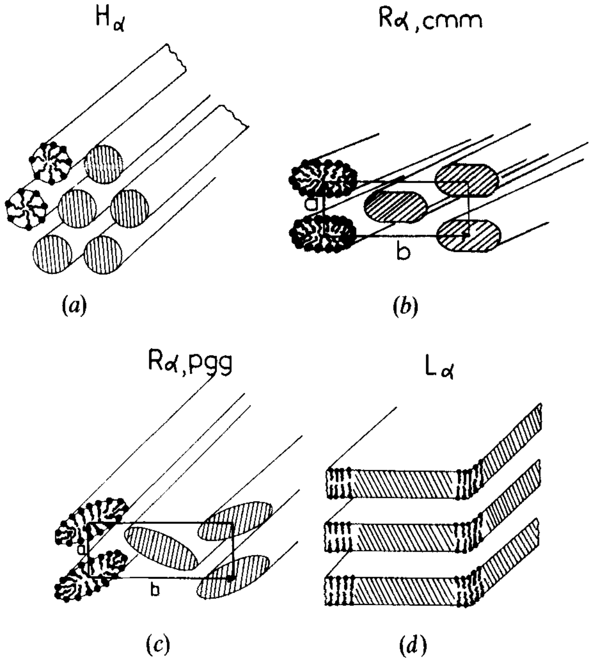

Figure 13. Sequence of mesophases along line A of the phase diagram (see figure 1) with increasing decanol content.

4. Summary

When sodium decyl sulphate molecules are progressively replaced by decanol molecules in the hexagonal phase of the SdS/H_2O system, the circular normal section of the cylindrical aggregates becomes rapidly distorted in an anisotropic manner and this anisotropy increases with the decanol/soap ratio, r. Above a certain value of the decanol/soap ratio, r, the anisotropy level becomes too high and the hexagonal phase transforms into a rectangular cmm phase which exists over a narrow domain of increasing r values and transforms rapidly in a rectangular pgg phase. The aggregates of both rectangular phases are infinite ribbons with non-circular section, i.e. their interfacial curvature is no longer homogeneous. We may infer that this inhomogeneity of the interfacial curvature is correlated with that of the distribution of the amphiphiles. Finally, still increasing the r ratio, the lamellar phase is reached but, just after the boundary of the domain the lamellae appear perturbed by the presence of structural defects, pores and/or channels which still imply strong curvature inhomogeneities. Clearly, as rectangular and lamellar phases are absent in the binary sodium decyl sulphate/water system this polymorphism is caused by the addition of decanol.

5. Concluding remarks

Two aspects will dominate this discussion: one concerns the shape and dimensions of the aggregates itself, the other concerns the ordering of the aggregates.

The normal section of the aggregates of the H_α phase does not remain circular when decanol is added. The shape of the section becomes anisotropic and aggregates with such anisotropic section do not have the six-fold symmetry of the lattice or a higher one, but this symmetry is presumably reached through an orientational disorder of the section of the aggregates along their long axis. Above a sufficiently high decanol concentration, $r > 0{\cdot}15$, the anisotropy of the section of the aggregates becomes large enough for the hexagonal phase to transform into a centred rectangular phase with cmm symmetry. Besides the direct experimental evidence for the anisotropy, it is clear that a circular isotropic growth of the section is impossible as it would require its radius to be much larger than the molecular length of an extended chain and, also, if the section was circular, the aggregates would come into contact along the shortest cell parameter.

In hexagonal phase, when the aggregates have anisotropic section, we assume that the six fold symmetry is reached through an orientational disorder of the sections of the aggregates along their long axis. Such a disorder probably subsists partially in the cmm R_α phase of lower symmetry. Owing to steric hindrance, the aggregates cannot perform 2π rotations along their long axis; however we may think that the cmm symmetry allows oscillations of the ribbons about a mean position.

The cmm phase extends over a narrow decanol concentration range, $0{\cdot}16 \leqslant r \leqslant 0{\cdot}18$ and transforms rapidly in a pgg phase. In both cases, cmm and pgg, the aggregates are infinite ribbons with flat and curved regions, and the aspect ratio of the normal section reaches 1·5. The interfacial amphiphilic/water curvature is inhomogeneous and its value integrated over the whole surface of a ribbon is intermediate between that of a cylinder with circular section, $1/R$, and that of a perfect lamella, zero. The parameters of the unit cell for the cmm and pgg phases are roughly of the same order of magnitude (see table 3) but the packing of the aggregates is different.

The pgg phase which extends for $0{\cdot}2 \leqslant r \leqslant 0{\cdot}27$ is characterized by a herring bone structure and we have determined the tilt angle of the aggregates to be about 9° (see figure 10). This structure results from the modifications of the intra-aggregate properties between the cmm and pgg phase, which are presumably at the origin of the modifications of the inter-aggregate properties. Indeed the increase of the decanol concentration, increases the inhomogeneity of the surface charge density of the aggregate whose section is anisotropic. In particular, as the SdS concentration is higher along the edges of the ribbon, its section can be depicted as a quadrupole. We may infer, that such a quadrupolar component in the electrostatic repulsive interactions between the aggregates, plays a role in the transformation of the cmm into a pgg rectangular phase. The herring bone type configuration with tilt angles of $\pm 9°$ of the aggregates in the pgg cell is energetically more favourable for quadrupoles than the parallel one of the cmm cell (see figure 13) and this may explain the latter exists only over a narrow domain.

When the decanol concentration is further increased $r \geqslant 0{\cdot}41$, a lamellar phase is reached, separated from the rectangular pgg phase by a polyphasic domain as shown in figure 1. The diffraction pattern (see figure 11 (*b*)) of the lamellar phase near the boundary of the polyphasic domain shows that the amphiphilic lamellae are perturbed by water inclusions which may be reminiscent of the ribbon-like structure of the rectangular phase [27]. When r is $\geqslant 0{\cdot}82$, the inclusions disappear and the amphiphilic lamellae are homogeneous, as usually described, up to $r = 3{\cdot}72$ which corresponds to the largest decanol/soap molar ratio we have investigated along line A (see figure 1).

It is quite noticeable that the change of the shape of the aggregates in the hexagonal phase, which starts at low decanol content, is not related to a change of the symmetry of the structure as long as r does not exceed 0·15. When the deformation of the cylinders which increases with the decanol content is sufficiently pronounced, it becomes a driving force for the transformation of the hexagonal phase into a rectangular cmm phase: the aggregates (ribbons) become organized with a lower symmetry on a rectangular lattice. The latter transforms rapidly into the more energetically favourable rectangular pgg structure. For a still higher decanol/soap ratio the lamellar phase appears. In the lower part of the lamellar domain, intra-layer modulations of density manifest themselves in the amphiphilic lamellae. They are not infinite and continuous but fragmented, presumably in ribbon-like aggregates [27]. This illustrates that a deformation of the ribbons into lamellae is not needed for the rectangular structure to change to a lamellar one.

Our description shows that, contrary to the general accepted description, the phase transformations are not necessarily related to changes of shapes and topologies. The symmetries of the aggregates and those of their organization are not necessarily related. Such a sequence can be put in parallel with sequences observed with thermotropic mesogens [28]. Several attempts have been made to develop theoretical descriptions of phase transitions observed for thermotropic mesogens. In particular, Carton *et al.* [29] discuss the different transitions in discotic columnar phases, from hexagonal to lower symmetry phases. The authors point out their model also applies to the deformation of columnar aggregates in lyotropic liquid crystals (p6m→cmm→pgg) which gives rise to a sequence of phase transformations such as those described in this paper.

References

[1] LUZZATI, V., MUSTACCHI, H., and SKOULIOS, A., 1958, *Discuss. Faraday Soc.*, **25**, 43.
[2] LUZZATI, V., MUSTACCHI, H., SKOULIOS, A., and HUSSON, F., 1960, *Acta crystallogr.*, **13**, 660.
[3] HUSSON, F., MUSTACCHI, H., and LUZZATI, V., 1960, *Acta crystallogr.*, **13**, 668.
[4] SKOULIOS, A., 1967, *Adv. Colloid Interf. Sci.*, **1**, 79.
[5] SKOULIOS, A., and LUZZATI, V., 1968, *Acta crystallogr.*, **19**, 278.
[6] LUZZATI, V., GULIK-KRZYWICKI, I., and TARDIEU, A., 1968, *Nature, Lond.*, **218**, 1031.
[7] EKWALL, P., 1975, *Advances in Liquid Crystals*, Vol. 1, edited by G. H. Brow (Academic Press), p. 1.
[8] CHARVOLIN, J., and TARDIEU, A., 1978, *Lyotropic Liquid Crystals, Structure and Molecular Motions*, Vol. 14, Solid State Physics, edited by F. Seitz and D. Turnbull (Academic Press), p. 209.
[9] KÉKICHEFF, P., and CABANE, B., 1987, *J. Phys., Paris*, **48**, 1571.
[10] KÉKICHEFF, P., and CABANE, B., 1988, *Acta crystallogr.*, **B44**, 395.
[11] MITCHELL, D. J., TIDDY, G., WARING, L., BOSTOCK, T., and MCDONALD, M. P., 1983, *J. chem. Soc. Faraday Trans.* 1, **79**, 975.
[12] RANÇON, Y., and CHARVOLIN, J., 1988, *J. phys. Chem.*, **92**, 2646.
[13] HENDRIKX, Y., and CHARVOLIN, J., 1981, *J. Phys., Paris*, **42**, 1427.
[14] ALPÉRINE, S., 1988, Thesis, Université Paris-Sud, Orsay.
[15] ALPÉRINE, S., HENDRIKX, Y., and CHARVOLIN, J., 1985, *J. Phys. Lett., Paris*, **46**, L-27.
[16] ROSEVAER, F. B., 1988, *J. Soc. Cosmet. Chem.*, **19**, 581.
[17] DE VRIES, J. J., and BERENDSEN, M. J. C., 1969, *Nature, Lond.*, **221**, 1139.
[18] HENDRIKX, Y., CHARVOLIN, J., and RAWISO, M., 1984, *J. Colloid Interf. Sci.*, **100**, 597.
[19] HENDRIKX, Y., and CHARVOLIN, J., 1988, *Liq. Crystals.*, **3**, 205.
[20] HENDRIKX, Y., CHARVOLIN, J., and RAWISO, M., 1986, *Phys. Rev.* B, **33**, 534.
[21] DOUCET, J., Laboratoire de Physique des Solides, Orsay (private communication).
[22] WARD, A. J., FRIBERG, S. E., LARSEN, W., and RANANANAVE, S. B., 1984, *J. phys. Chem.*, **88**, 826.
[23] LUZZATI, V., 1968, *Biological Membranes*, edited by D. Chapman, (Academic Press), p. 77.
[24] HOLMES, M. C., and CHARVOLIN, J., 1984, *J. phys. Chem.*, **88**, 810.
[25] HOLMES, M. C., CHARVOLIN, J., and REYNOLDS, D. J., 1988, *Liq. Crystals.*, **3**, 114.
[26] KÉKICHEFF, P., CABANE, B., and RAWISO, M., 1984, *J. Phys. Lett., Paris*, **45**, 813.
[27] HENDRIKX, Y., CHARVOLIN, J., KÉKICHEFF, P., and ROTH, M., 1987, *Liq. Crystals.*, **2**, 677.
[28] HENDRIKX, Y., and LEVELUT, A. M., 1988, *Molec. Crystal liq. Crystals*, **165**, 235.
[29] CARTON, J. P., DUBOIS-VIOLETTE, E., and PROST, J., 1990, *Liq. Crystals*, **4**, 305.